ARTICLE
Journal of Cellular Biochemistry 112:3732–3741 (2011)

Journal of Cellular Biochemistry

The Neuropeptide VIP Regulates the Expression of Osteoclastogenic Factors in Osteoblasts

Emma Persson[1] and Ulf H. Lerner[1,2*]

[1]*Division of Molecular Periodontology, Umeå University, Umeå, Sweden*

[2]*Centre for Bone and Arthritis Research, Institute of Medicine, Sahlgrenska Academy, University of Gothenburg, Gothenburg, Sweden*

ABSTRACT

Osteoclast formation is controlled by stromal cells/osteoblasts expressing macrophage colony-stimulating factor (M-CSF) and receptor activator of NF-κB ligand (RANKL), crucial for osteoclast progenitor cell proliferation, survival and differentiation, and osteoprotegerin (OPG) that inhibits the interaction between RANKL and its receptor RANK. Recent data have strongly indicated that the nervous system plays an important role in bone biology. In the present study, the effects of the neuropeptide vasoactive intestinal peptide (VIP), present in peptidergic skeletal nerve fibers, on the expression of RANKL, OPG, and M-CSF in osteoblasts and stromal cells have been investigated. VIP and pituitary adenylate cyclase-activating polypeptide 38 (PACAP-38), but not secretin, stimulated *rankl* mRNA expression in mouse calvarial osteoblasts. In contrast, VIP inhibited the mRNA expressions of *opg* and *m-csf*, effects shared by PACAP-38, but not by secretin. VIP did not affect *rankl*, *opg*, or *m-csf* mRNA expression in mouse bone marrow stromal cells (BMSCs). The effects by VIP on the mRNA expression of *rankl*, *opg*, and *m-csf* were all potentiated by the cyclic AMP phosphodiesterase inhibitor rolipram. In addition, VIP robustly enhanced the phosphorylation of ERK and the stimulatory effect by VIP on *rankl* mRNA was inhibited by the MEK1/2 inhibitor PD98059. These observations demonstrate that activation of $VPAC_2$ receptors in osteoblasts enhances the RANKL/OPG ratio by mechanisms mediated by cyclic AMP and ERK pathways suggesting an important role for VIP in bone remodeling. J. Cell. Biochem. 112: 3732–3741, 2011.

KEY WORDS: VIP; RANKL; OSTEOBLAST; BONE

Immunohistochemical studies have demonstrated a network of peptidergic nerve fibers in the skeleton [Bjurholm et al., 1989; Hill and Elde, 1990]. The close proximity between nerve endings and bone cells [Imai et al., 1997], and the increased density of skeletal nerve fibers in areas with high metabolic activity such as the growth plate [Hukkanen et al., 1993], growing antlers [Gray et al., 1992], and the callus of healing skeletal fractures [Madsen et al., 1998] have suggested that the signaling molecules in skeletal nerve fibers not only have sensory functions but may also participate in the control of bone cell activities [reviewed in Lerner et al., 2008]. Such a possibility is supported by findings demonstrating that nerve deletions result in changes in osteoblast and osteoclast activities [Hill and Elde, 1991; Cherruau et al., 1999]. Recently, the importance of the central nervous system for skeletal remodeling has been elegantly demonstrated by the observations that brain stem receptors for leptin are linked to regulation of bone formation and resorption by serotonergic signaling to hypothalamus and downstream sympathetic control of β-adrenergic receptors on osteoblasts [Yadav et al., 2009; Ducy and Karsenty, 2010]. Also hypothalamic NPY receptors have been demonstrated to regulate bone mass [reviewed in Wong et al., 2008].

Vasoactive intestinal peptide (VIP) is a neuropeptide expressed in peptidergic skeletal nerve fibers [Hohmann et al., 1986; Bjurholm et al., 1988; Hill and Elde, 1991]. Our group and others have shown that osteoblasts and osteoclasts are equipped with different functional VIP receptor subtypes, as assessed by cyclic AMP formation, reverse transcriptase polymerase chain reaction (RT-PCR), radioligand binding, and atomic force microscopy [Hohmann et al., 1983; Hohmann and Tashjian, 1984; Bjurholm et al., 1992; Lerner et al., 1994; Togari et al., 1997; Lundberg et al., 2000, 2001; Ransjö et al., 2000]. Mouse calvarial osteoblasts express VIP type 2 receptors ($VPAC_2$ receptors) and activation of these receptors causes increased expression of alkaline phosphatase and enhanced mineralization of osteoblastic bone nodules in vitro [Lundberg et al., 1999], without

Additional supporting information may be found in the online version of this article.

Emma Persson's present address is Department of Radiation Sciences, Oncology, Umeå University, Umeå, Sweden.
*Correspondence to: Prof. Ulf H. Lerner, Division of Molecular Periodontology, Umeå University, S-901 87 Umeå, Sweden. E-mail: ulf.lerner@odont.umu.se

Received 14 February 2011; Accepted 28 July 2011 • DOI 10.1002/jcb.23304 • © 2011 Wiley Periodicals, Inc.
Published online 3 August 2011 in Wiley Online Library (wileyonlinelibrary.com).

affecting the expression of type I α1 collagen or osteocalcin [Lundberg et al., unpublished data].

Osteoblasts, however, not only are important for bone matrix biosynthesis and mineralization, but also secrete a variety of cytokines, some of which are important for osteoclast proliferation, survival, and differentiation. We have previously observed that VIP enhances interleukin-6 (IL-6) expression and release from mouse calvarial osteoblasts, without affecting those of IL-11, leukemia inhibitory factor (LIF) or oncostatin M [Persson et al., 2005]. We also have shown that VIP potentiates the stimulatory effect of several osteotropic, proinflammatory cytokines on IL-6 expression in mouse calvarial osteoblasts [Persson and Lerner, 2005].

Macrophage colony-stimulating factor (M-CSF) is a cytokine released by osteoblasts which by activation of its cognate receptor c-Fms is important for osteoclast proliferation and survival [reviewed in Ross and Teitelbaum, 2005; Lorenzo et al., 2008]. Its prominent role in bone metabolism is demonstrated in the *op/op* mouse in which absence of functional M-CSF due to a thymidine insertion in the M-CSF gene results in osteopetrosis as a consequence of severe deficiency of osteoclasts [Yoshida et al., 1990] and by the fact that lack of c-Fms due to gene deletion results in an osteopetrotic phenotype in mice [Dai et al., 2002].

Receptor activator of NF-κB ligand (RANKL) is a type II transmembrane cytokine in the tumor necrosis factor (TNF) ligand superfamily that is expressed by osteoblasts in periosteum and stromal cells in bone marrow. RANKL activates the cognate receptor RANK on osteoclast progenitor cells and thereby stimulates the differentiation of the progenitor cells to cells that can fuse to multinucleated osteoclasts [reviewed in Lerner, 2004; Lorenzo et al., 2008; Nakashima and Takayanagi, 2009]. Osteoprotegerin (OPG), which similar to RANK is a member of the TNF receptor superfamily, functions as a soluble decoy receptor, which due to its affinity to RANKL inhibits RANK activation and osteoclast formation. Deletion of the genes for RANKL and RANK results in a lack of osteoclasts and an osteopetrotic phenotype in mice [Dougall et al., 1999; Kong et al., 1999], whereas $opg^{-/-}$ mice exhibit an abundance of osteoclasts and an osteoporotic phenotype [Bucay et al., 1998]. In humans, gain-of-function mutation in the *rank* gene has been linked to two diseases with increased osteoclastic bone resorption; familial expansive osteolysis and expansive skeletal hyperphosphatasia [Hughes et al., 2000; Whyte and Hughes, 2002; Johnson-Pais et al., 2003]. Deletion of the gene encoding *opg* has been associated with increased number of osteoclasts observed in patients with *hyperostosis corticalis deformans juvenilis* [Whyte et al., 2002].

In the present investigation, we have studied the effect of VIP and related peptides in the VIP/secretin/glucagon family of peptides, on the expression of RANKL, OPG, and M-CSF in mouse calvarial osteoblasts and bone marrow stromal cells (BMSCs), as well as in the mouse, rat, and human osteoblastic cell lines MC3T3-E1, ROS 17/2.8, UMR-106, MG-63, and SaOS-2.

MATERIALS AND METHODS

MATERIALS

Synthetic VIP was purchased from Bachem, Bubendorf, Switzerland; pituitary adenylate cyclase-activating polypeptide 38 (PACAP-38) and secretin from Peninsula, St. Helens, Merseyside, UK; α modification of minimum essential medium (α-MEM), fetal bovine serum (FBS), L-glutamine, and oligonucleotide primers from Invitrogen, Stockholm, Sweden; mouse RANKL ELISA kit from R&D Systems, Abingdon, UK; prostaglandin E_2 (PGE_2), cAMP RIA kit from Perkin Elmer, Boston, MA; 1st strand cDNA synthesis Kit and PCR Core Kit from Roche, Mannheim, Germany; RNAqueous 4-PCR kit from Ambion Inc., Austin, TX; DYEnamic ET terminator cycle sequencing kit from Amersham Biosciences, Uppsala, Sweden; TaqMan Universal PCR Master Mix and TaqMan probes from Applied Biosystems, Foster City, CA; anti-Actin (I-19) and anti-P-ERK1/2 (E-4) primary antibodies were from Santa Cruz Biotechnology, Inc., Santa Cruz, CA; anti-IgG-HRP secondary antibodies used for Western blot were from Dakopatts, Glostrup, Denmark; PD98059 from Sigma–Aldrich, Stockholm, Sweden; culture dishes and multi-well plates from Costar, Cambridge, MA; 1,25-dihydroxyvitamin D_3 (D3) from Hoffmann-LaRoche, Basel, Switzerland. Rolipram was kindly supplied by Dr. Sprzgala from Schering AG, Berlin, Germany.

ANIMALS

CsA mice from our own inbred colony were used for all experiments. Animal care and experiments were approved and conducted in accordance with accepted standards of humane animal care and use as deemed appropriate by the Animal Care and Use Committee of Umeå University, Umeå, Sweden.

MOUSE CALVARIAL OSTEOBLAST ISOLATION

Bone cells were isolated from calvariae from 2 to 3 day-old CsA mice using a modified time sequential enzyme-digestion technique [Boonekamp et al., 1984]. Cells from populations 6–10, showing an osteoblastic phenotype as assessed by their cyclic AMP-responsiveness to PTH, expression of alkaline phosphatase, osteocalcin, and bone sialoprotein, as well as the capacity to form mineralized bone nodules (data not shown), were used. The cells were seeded in culture flasks containing α-MEM supplemented with 10% FBS, L-glutamine and antibiotics at 37°C in humidified air containing 5% CO_2. After 4 days in flasks, the cells were detached and seeded in multi-well plates for the different experiments. For gene expression analyses, osteoblasts were plated at a density of $3–5 \times 10^4$ cells/cm^2, and after attachment overnight, cells were cultured in α-MEM containing 10% FBS, L-glutamine, and antibiotics, with or without test substances for 12–120 h. For semi-quantitative PCR, cells were seeded in 9 cm^2 culture wells and two culture wells per treatment group were used from which RNA was pooled. For quantitative real-time PCR, cells were seeded in 4.5 cm^2 culture wells and 3–4 wells per treatment group were used. For cyclic AMP experiments, osteoblasts were seeded at a density of $6–8 \times 10^4$/cm^2 in 2 cm^2 wells and four wells per treatment groups were used.

CULTURE OF OSTEOBLASTIC CELL LINES MC3T3-E1, ROS 17/2.8, UMR 106-01, MG-63, AND SaOS-2

The mouse, non-transformed cell line MC3T3-E1, the rat osteosarcoma cell lines ROS 17/2.8 and UMR 106-01, and the human osteosarcoma cell lines MG-63 and SaOS-2 were cultured in α-MEM supplemented with 10% FBS, L-glutamine and antibiotics at 37°C in humidified air containing 5% CO_2. Following an initial growth

period with media change every 2 days, cells were seeded at a density of $3–5 \times 10^4$ cells/cm^2 in 9 cm^2 wells. After attachment overnight, cells were incubated for gene expression analysis in α-MEM containing 10% FBS, L-glutamine and antibiotics with or without (control) test substances for 48 h. Three culture wells per treatment group were used from which RNA were pooled.

ISOLATION OF MOUSE BONE MARROW STROMAL CELLS

The femurs and tibiae from 5 to 7 weeks old male mice were dissected and cleaned from adhering tissues. The cartilage ends were cut off and the cells in the marrow cavity were flushed out by α-MEM in a syringe with a sterile needle. The marrow cells were collected in α-MEM/10% FBS and the erythrocytes lysed in red blood cell lysis buffer (0.16 M NH_4Cl, 0.17 M Tris, pH 7.65). Cells from 4 to 8 bones were seeded in one 60 cm^2 culture dish and incubated in α-MEM/10% FBS with no hormones or cytokines added. After 4–8 days, with a change of medium after 2 and 4 days, the adherent cells were carefully washed and then detached and seeded at a density of 10^4 cells/cm^2 in α-MEM containing 10% FBS, L-glutamine and antibiotics, with or without (control) test substances for 12–120 h for gene expression studies. The BMSCs obtained expressed mRNA for *akp1*, *ocn*, *rankl*, *opg*, but not for *rank*, *ctsk*, *acp5*, or *calcr* (data not shown). The BMSC formed mineralized bone noduli when cultured in the presence of β-glycerophosphate (data not shown). In addition, BMSC were seeded at a density of $6–8 \times 10^4$ cells/cm^2 in 2 cm^2 wells and used for assessment of cyclic AMP formation as described below.

CYCLIC AMP ACCUMULATION IN CALVARIAL OSTEOBLASTS AND BONE MARROW STROMAL CELLS

Calvarial osteoblasts or BMSC isolated and seeded as described above were grown to 80–90% confluency. Then, the cells were washed in serum-free medium and pre-incubated at 37°C for 30 min in serum-free HEPES-buffered α-MEM added the cyclic AMP phosphodieserase inhibitor rolipram (10^{-5} M). Subsequently, medium without (controls) or with PGE_2 (10^{-5} M), VIP (10^{-6} M), PACAP-38 (10^{-6} M), or secretin (10^{-6} M) was added and cells incubated for 2, 5, or 15 min. At the end of the experiments, the media were withdrawn and cellular cyclic AMP extracted with 90% n-propanol. The samples were then evaporated under vacuum, reconstituted in assay buffer and cyclic AMP quantified using a commercially available RIA kit.

RNA ISOLATION AND cDNA SYNTHESIS

Total RNA was extracted from calvarial osteoblasts, BMSC, or osteoblastic cells lines by using the RNAqueous 4-PCR kit by following the manufacturer's protocol. The RNA was quantified spectrophotometrically and the integrity of the RNA preparations was examined by agarose gel electrophoresis. Only RNA from intact preparations were used for subsequent analysis. One microgram of total RNA was reverse transcribed into single-stranded cDNA with a 1st Strand cDNA Synthesis Kit using oligo-$p(dT)_{15}$ primers. After incubation at 25°C for 10 min and at 42°C for 60 min, the AMV reverse transcriptase was denaturated at 99°C for 5 min. The cDNA was kept at −20°C until used for PCR.

SEMI-QUANTITATIVE RT-PCR

Synthesized cDNA was amplified by RT-PCR using a PCR Core Kit and PC-960G Gradient Thermal Cycler (Corbett Research, Australia), and the PCRs for mouse, rat, and human *rankl*, *opg*, and *m-csf* were performed using standard protocol. For all primers except mouse *rankl* and *opg*, the reaction conditions were: denaturing at 94°C for 2 min, annealing for 40 s followed by elongation at 72°C for 90 s; in subsequent cycles denaturing was performed at 94°C for 40 s. For mouse *rankl* and *opg*, the annealing temperature started at 65°C for 10 cycles, followed by stepwise decrease 5°C every five cycles from 65 to 45°C. The sequences of primers used, the GenBank accession numbers, annealing temperature, and estimated sizes of the PCR products are given in supplemental material. The expression of these factors was compared at the logarithmic phase of the PCR reaction. No amplification was detected in samples where the RT reaction had been omitted (data not shown). The PCR products were electrophoretically size fractionated in 1.5% agarose gel and visualized using ethidium bromide. The identity of the PCR products was confirmed using a DYEnamic ET^{TM} terminator cycle sequencing kit with sequences analyzed on an ABI 377 XL DNA Sequencer (PE Applied Biosystems, Foster City, CA).

QUANTITATIVE REAL-TIME PCR

Quantitative real-time PCR analyses of *rankl*, *opg*, *m-csf*, *36b4*, and *β-actin* mRNA were performed using TaqMan kinetics and cDNA diluted 1:20 in nuclease free water. For all except *m-csf*, TaqMan Universal PCR Master Mix kit, 300 nM of each primer and 100 nM of probe were used. For *m-csf*, an assay-on-demand mix with both primers and probe was used (Applied Biosystems, Foster City, CA). All analyses were performed using an ABI PRISM 7900 HT Sequence Detections System and software (Applied Biosystems, Foster City, CA). The reaction conditions were an initial step of 2 min at 50°C and 10 min at 95°C for 15 s, followed by 40 cycles of denaturation at 95°C for 15 s and annealing/extension at 60°C for 1 min. The sequences of primers and probes and the GenBank accession numbers are shown in supplemental material. To control for variability in amplification due to differences in starting mRNA concentrations, β-actin, or the ribosomal phosphoprotein 36B4 was used as an internal standard. The relative expression of target mRNA was computed from the target Ct values and β-actin or 36B4 Ct values using the standard curve method.

PREPARATION OF TOTAL CELL LYSATES

Calvarial osteoblasts were seeded in 60 cm^2 dishes at a density of 2×10^4 cells/cm^2. After 3 days of culture with one media change, the cells were incubated in the absence (control) or presence of test substances for different time periods. Following incubation, the cells were washed twice in PBS before addition of lysis buffer (1% Igepal CA-630, 0.1% SDS, 2 mM EDTA, 50 mM NaF, 0.1 mg/ml PMSF, 10 μg/ml leupeptin, 10 μg/ml pepstatin A in PBS). The dishes were kept on ice for 15 min followed by scraping and collection of cell lysates. Before use in Western blot, cell lysates were concentrated using Microcon centrifugal filter devices according to manufacturer's recommendations. Protein concentration of the cell lysates was measured using the BCA method with bovine albumin as standard.

WESTERN BLOT ANALYSIS

For Western blot analysis, cell lysates were mixed with sample buffer (200 mM Tris-HCl, pH 6.7, 20% glycerol, 10% β-mercaptoethanol, 5% SDS, 0.01% Pyronin Y) and boiled for 3 min. Protein samples were then loaded on 12% Tris-HCl polyacrylamide gels and electrophoresis was performed according to the Laemmli method. Electrophoresed proteins were then blotted onto a polyvinylidene fluoride (PVDF) membrane which was blocked (1% milk, 1% BSA in TBS) overnight. For detection, the membrane was incubated with primary antibody (1:200 in 1% milk, 1% BSA, 0.05% Tween-20 in TBS) for 60 min at room temperature. Three times 10 min of wash in TBS with 0.05% Tween-20 (TBST) was followed by incubation with HRP-conjugated secondary antibody (1:1,000 in 1% milk, 1% BSA, 0.05% Tween-20 in TBS) for 60 min at room temperature. Finally, the membrane was washed extensively with TBST and TBS followed by development using a chemiluminescence detection kit according to manufacturer's protocol.

STATISTICAL ANALYSIS

Statistical significance was determined by ANOVA including Dunnett's two-sided or Dunnett's T3 post hoc test. Numerical values are expressed as percent of unstimulated control, controls presented as 100% if not otherwise stated. Data are expressed as mean ± SEM and SEM is shown when the height of the error bar is larger than the height of the symbol.

RESULTS

VIP STIMULATES RANKL mRNA AND INHIBITS OPG AND M-CSF mRNA IN MOUSE CALVARIAL OSTEOBLASTS BY A CYCLIC AMP DEPENDENT PATHWAY

Quantitative real-time PCR analysis showed that treatment of mouse calvarial osteoblasts for 48 h with VIP (10^{-6} M) significantly increased *rankl* mRNA expression (Fig. 1A) and decreased mRNA expression of *opg* (Fig. 1B). The mRNA expression of *m-csf* was reduced by VIP, but did not reach statistical significance (Fig. 1C). The reduction was, however, reproducibly seen in several individual experiments (see also Figs. 1F, 2A, and 3). The concentration of VIP used (10^{-6} M), was based upon previous studies showing that mouse calvarial osteoblasts respond to VIP in terms of cyclic AMP formation at and above 10^{-9} M, and that 10^{-6} M is near the maximally effective concentration [Lundberg et al., 2001].

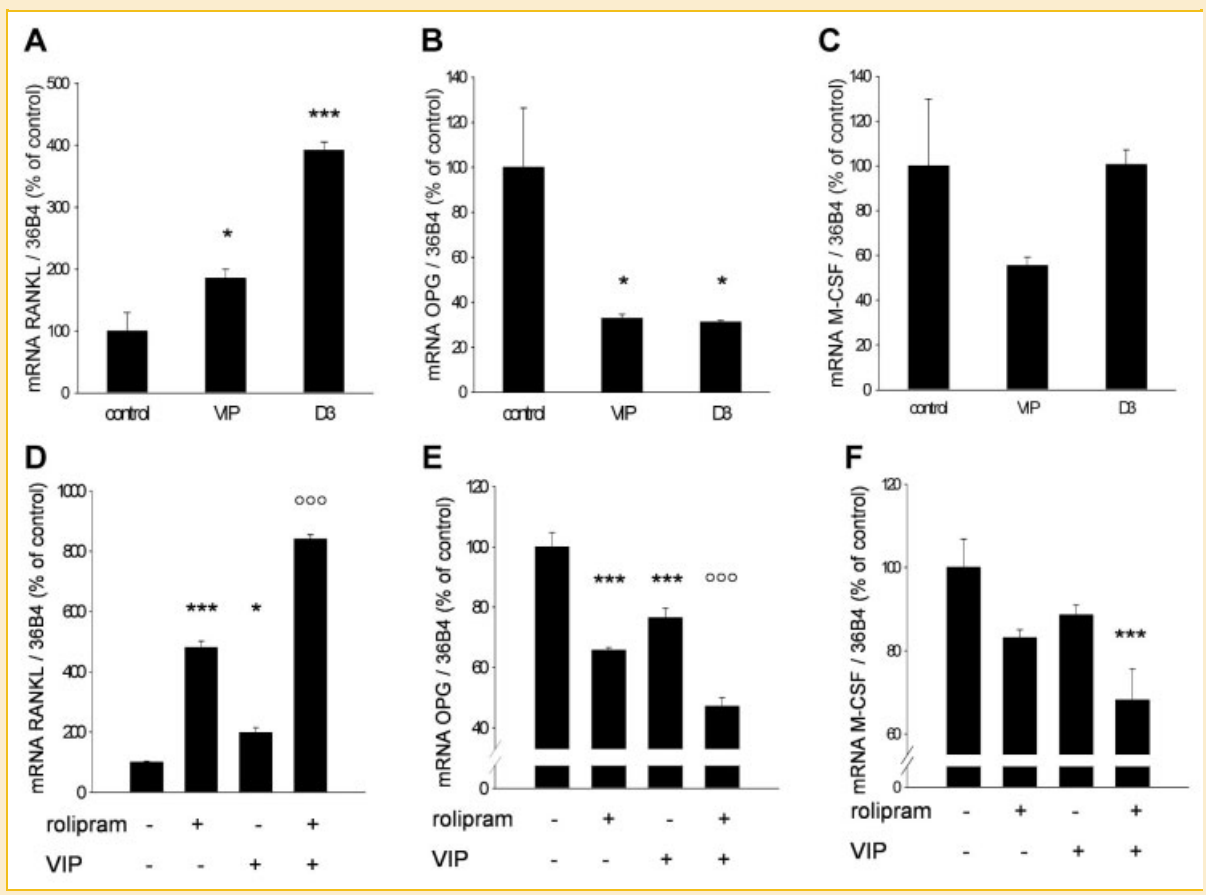

Fig. 1. VIP regulates mRNA expressions of both osteoclastogenic and anti-osteoclastogenic factors by a mechanism mediated by the cyclic AMP/protein kinase A pathway. Calvarial osteoblasts were cultured in the absence (control) or presence of either VIP (10^{-6} M) or D3 (10^{-9} M)(A–C) or with VIP (10^{-6} M) without or with the phosphodiesterase inhibitor rolipram (10^{-5} M) for 48 h before RNA isolation and quantitative real-time PCR analysis of *rankl* (A, D), *opg* (B, E), and *m-csf* (C, F) mRNA expressions. The values for untreated cells are defined as controls and presented as 100%. Samples were analyzed in triplicates and normalized with 36B4. * and ***, indicates significant difference compared to untreated cells, $P < 0.05$ and $P < 0.001$, respectively. °°°, indicates significant difference of VIP in combination with rolipram compared to VIP alone, $P < 0.001$.

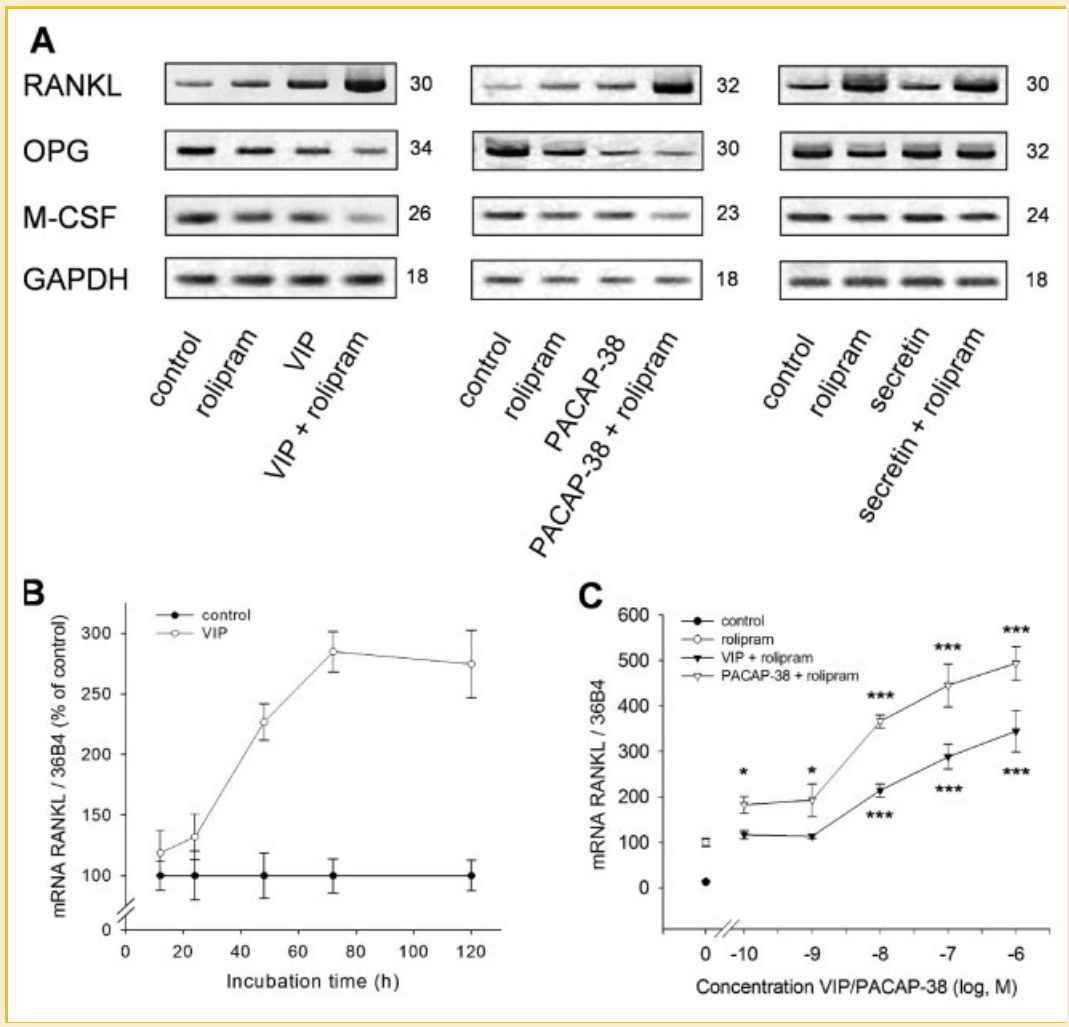

Fig. 2. VIP and PACAP-38 stimulates *rankl* mRNA and inhibits *opg* and *m-csf* mRNA expression through a mechanism mediated by $VPAC_2$ receptors. Isolated calvarial osteoblasts were incubated in the absence (control) or presence of VIP, PACAP-38, secretin, and the phosphodiesterase inhibitor rolipram. A: Semiquantitative RT-PCR analysis after incubation without (control) or with VIP, PACAP-38 and secretin (all at 10^{-6} M) in the absence or presence of rolipram (10^{-5} M) for 48 h. The RT-PCR expressions were normalized with GAPDH. Numbers indicates number of PCR cycles. B: Quantitative real-time PCR analysis of *rankl* mRNA expression in osteoblasts cultured in the absence (control) or presence of VIP (10^{-6} M) for 12–120 h. The values for untreated cells are defined as controls and are presented as 100%. C: Quantitative real-time PCR analysis of *rankl* mRNA from calvarial osteoblasts treated with rolipram (10^{-5} M) or rolipram together with different concentrations of VIP or PACAP-38. In quantitative PCR reactions, samples were analyzed in triplicates and normalized with 36B4. The values for untreated cells are defined as controls, the values for cells treated with rolipram are presented as 100%. * and ***, indicates significant difference of VIP/PACAP-38 in combination with rolipram compared to rolipram alone, $P < 0.05$ and $P < 0.001$, respectively.

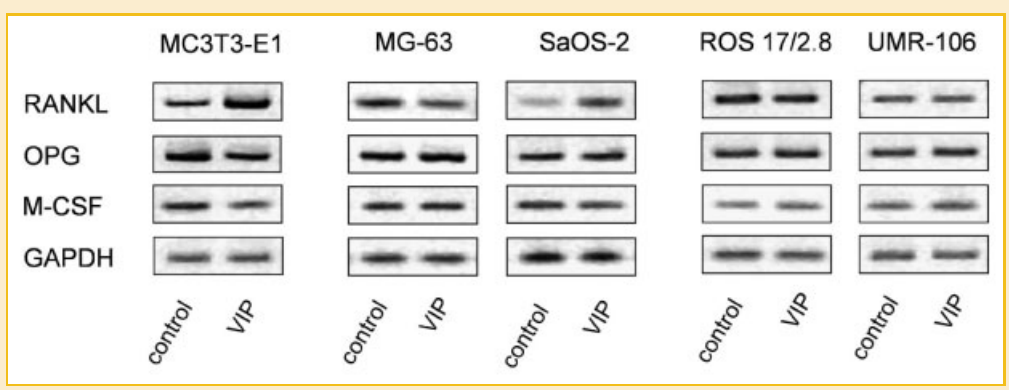

Fig. 3. Regulation of *rankl*, *opg*, and *m-csf* mRNA expression by VIP in mouse, rat, and human osteoblastic cell lines. Cells from the murine osteoblastic cell line MC3T3-E1, the human osteosarcoma cell lines MG-63 and SaOS-2, and the rat osteosarcoma cell lines ROS 17/2.8 and UMR 106-01 were incubated without (control) or with VIP (10^{-6} M) for 48 h before semi-quantitative RT-PCR analyses of *rankl*, *opg*, and *m-csf* mRNA expressions were performed. The RT-PCR expressions were normalized with GAPDH.

1,25-dihydroxyvitamin D_3 (D3; 10^{-9} M), used as a positive control, increased *rankl* mRNA and inhibited *opg* mRNA (Fig. 1A, B), as expected. 1,25-dihydroxyvitamin D_3 did not affect *m-csf* mRNA after 48 h of incubation (Fig. 1C). However, at earlier time points (12–24 h), D3 caused a significant ($P < 0.05$), 1.5- to 3-fold enhancement of *m-csf* mRNA (unpublished data). Attempts were made to perform RANKL protein analysis using ELISA, but the amounts of RANKL protein in cell lysates and conditioned media were below the detection limit.

Stimulation of *rankl* mRNA and inhibition of *opg* and *m-csf* mRNA by VIP (10^{-6} M) were all potentiated by the cyclic AMP phosphodiesterase inhibitor rolipram (10^{-5} M; Fig. 1D–F).

THE EFFECTS OF VIP ON RANKL, OPG, AND M-CSF mRNA IN MOUSE CALVARIAL OSTEOBLASTS ARE MEDIATED BY VIP TYPE 2 RECEPTORS

Stimulation of mouse calvarial osteoblasts for 48 h with either VIP or PACAP-38, at concentrations of 10^{-6} M, increased mRNA expression of *rankl* as assessed by semi-quantitative RT-PCR, an effect that was potentiated by the cyclic AMP phosphodiesterase inhibitor rolipram (10^{-5} M; Fig. 2A). Secretin (10^{-6} M), however, did not affect *rankl* mRNA, neither in the absence nor in the presence of rolipram (Fig. 2A). The mRNA expression of *opg* was decreased by VIP and PACAP-38, effects that were potentiated by rolipram (Fig. 2A), whereas secretin did not have any effect, neither in the absence nor presence of rolipram (Fig. 2A). Furthermore, treatment with VIP or PACAP-38, but not secretin, resulted in a slight decrease of *m-csf* mRNA levels, and the effects were further potentiated by rolipram (Fig. 2A).

Stimulation of *rankl* mRNA by VIP (10^{-6} M) was dependent on time with enhancement observed at 12 h, an effect which gradually increased with time for 72 h and remained elevated at least for 120 h (Fig. 2B). The effects of VIP and PACAP-38 on *rankl* mRNA were concentration dependent with PACAP-38 slightly (10-fold) more potent than VIP and, in addition, also slightly more effective at optimal concentrations (Fig. 2C). The fact that secretin did not have any effect on the transcription of neither of the genes studied, and that VIP and PACAP-38 had effects with similar potency, indicates that the effects are mediated by $VPAC_2$ receptors. These observations are in agreement with our previous findings showing that mouse calvarial osteoblasts express $VPAC_2$ receptors as assessed by radioligand binding, atomic force microscopy, and cyclic AMP response to peptides preferring $VPAC_2$ but not $VPAC_1$ or PAC_1 receptors [Lundberg et al., 2001]. We also showed that these cells expressed mRNA for $VPAC_2$, but not for $VPAC_1$ or PAC_1 receptors.

EFFECT OF VIP ON RANKL, OPG, AND M-CSF mRNA EXPRESSIONS IN THE OSTEOBLASTIC CELL LINES MC3T3-E1, ROS 17/2.8, UMR 106-01, MG-63, AND SaOS-2

To further evaluate the role of VIP as a regulator of RANKL, OPG, and M-CSF expressions in osteoblasts we studied the effects in the mouse osteoblastic cell lines MC3T3-E1, the rat osteoblastic cell lines ROS 17/2.8 and UMR 106-01 and in the human osteoblastic cell lines MG-63 and SaOS-2 after incubation of the cells without or with VIP (10^{-6} M) for 48 h. In MC3T3-E1 cells, incubation with VIP resulted in increased *rankl* mRNA expression, whereas the levels of *opg* and *m-csf* mRNA were decreased (Fig. 3), results similar to those obtained in primary calvarial osteoblasts (Fig. 1A–C). In the human osteosarcoma cell line SaOS-2, incubation with VIP increased the mRNA expression of *RANKL* (Fig. 3), similar to the results in mouse calvarial osteoblasts and the cell line MC3T3-E1. At variance, incubation with VIP caused a decrease in *RANKL* mRNA levels in the human osteoblastic cell line MG-63 (Fig. 3). In contrast to the regulation of *RANKL* mRNA, expression of *OPG* and *M-CSF* mRNA were not regulated by VIP in SaOS-2 or MG-63 cells (Fig. 3). In addition, neither r*ankl*, nor *opg*, or *m-csf* mRNA were regulated by VIP in the rat osteosarcoma cell lines ROS 17/2.4 and UMR 106-01 (Fig. 3).

VIP DOES NOT REGULATE RANKL, OPG, OR M-CSF IN MOUSE BONE MARROW STROMAL CELLS (BMSC)

VIP (10^{-6} M) did not affect *rankl* (Fig. 4A), *opg* (Fig. 4B), or *m-csf* (Fig. 4C) mRNA in mouse BMSC over a time period of 12–120 h. In contrast, D3 (10^{-9} M) increased *rankl* mRNA and decreased *opg* mRNA, as expected (Fig. 4A, B). The lack of effect by VIP (10^{-6} M) on *rankl* and *opg* mRNA were seen also in three additional 48 h experiments in which D3 caused the anticipated stimulation of *rankl* and inhibition of *opg* mRNA (unpublished data). Surprisingly, *m-csf* mRNA was not increased by D3 in the BMSC, but rather decreased after a delay of 48 h (Fig. 4C).

EFFECTS OF VIP, PACAP-38, AND SECRETIN ON CYCLIC AMP ACCUMULATION IN MOUSE CALVARIAL OSTEOBLASTS AND BONE MARROW STROMAL CELLS

VIP (10^{-6} M) and PACAP-38 (10^{-6} M), but not secretin (10^{-6} M), stimulated cyclic AMP accumulation in calvarial osteoblasts (Fig. 5A). In contrast, VIP, PACAP-38, and secretin did not affect cyclic AMP accumulation in BMSC (Fig. 5B). PGE_2 (10^{-5} M), used as a positive control, enhanced cyclic AMP accumulation in both calvarial osteoblasts and BMSC, although to a lesser degree in the BMSC (Fig. 5A, B).

THE EFFECT BY VIP ON RANKL EXPRESSION IS MEDIATED BY ERK

We have in a previous publication reported that the stimulatory effect by VIP on IL-6 expression in calvarial osteoblasts is mediated by several signaling pathways, including cyclic AMP/CREB, AP-1 and C/EBP [Persson et al., 2005]. In addition, Natsume et al. [2010] demonstrated that VIP in synergy with TNF-α increased IL-6 expression in osteoblastic MC3T3-E1 cells, an effect that was mediated by the ERK pathway. To further elucidate the mechanisms, besides cyclic AMP, that may be involved in regulation by VIP of RANKL expression, we also studied the possible activation of the ERK pathway. Indeed, incubation of calvarial osteoblasts in the presence of VIP for 15–30 min strongly induced phosphorylation of p42/p44 ERK proteins (Fig. 6A). In addition, calvarial osteoblasts were incubated for 48 h in the absence (control) or presence of VIP (10^{-6} M) or VIP + PD98059 (30 μM), a MEK1/2 inhibitor. The stimulatory effect by VIP on *rankl* mRNA expression was reversed by 60% in the presence of PD98059 (Fig. 6B). These findings, together, indicate that the stimulatory effect by VIP on *rankl* expression is, at least partly, mediated by the MEK/ERK pathway.

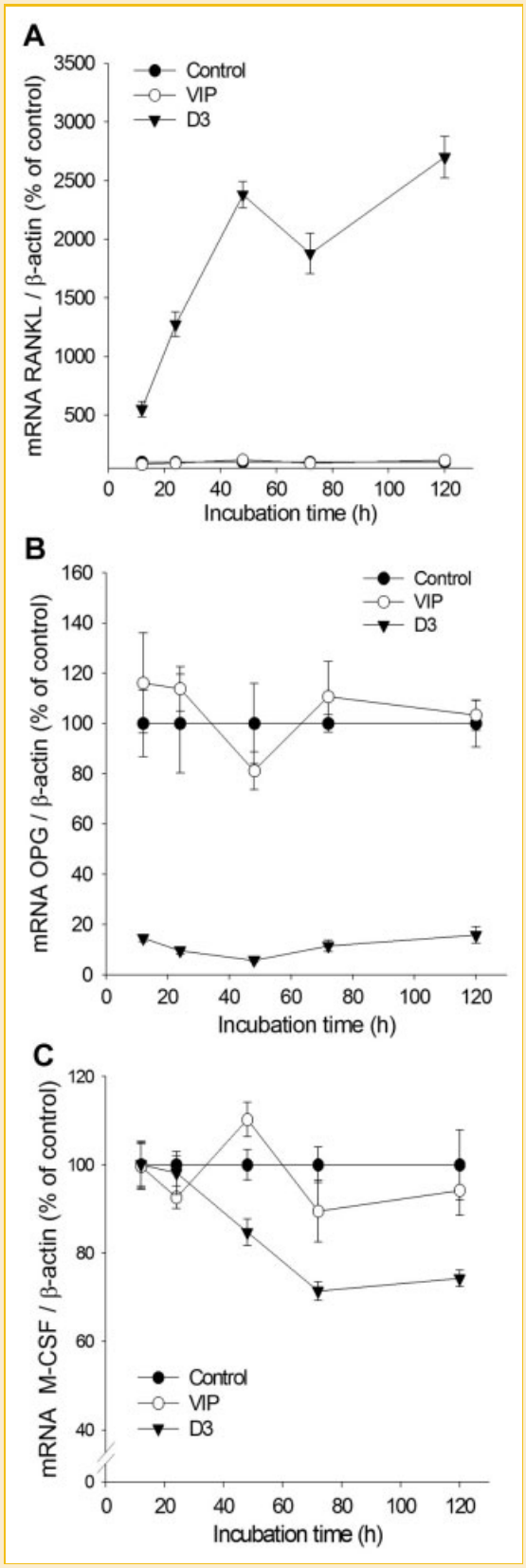

DISCUSSION

In order to assess whether activation of the VIP receptors present on osteoblasts [Lerner et al., 2008] may lead to regulation of the osteoclastogenic properties of osteoblasts, we have studied the effect of VIP on RANKL, OPG, and M-CSF in mouse calvarial osteoblasts, in several mouse, rat, and human osteoblastic cell lines, as well as in mouse BMSCs.

In primary cultures of mouse periosteal osteoblasts, and in the mouse osteoblastic cell line MC3T3-E1 (derived from mouse periosteal osteoblasts), VIP enhanced *rankl* and decreased *opg* and *m-csf* mRNA expression. In the human osteosarcoma cell line SaOS-2, VIP also enhanced *RANKL* mRNA, whereas in the human osteosarcoma cell line MG-63 *RANKL* mRNA expression was decreased by VIP. These observations indicate that SaOS-2 and MG-63 express functional VIP receptors, in line with our previous observations using cyclic AMP as a parameter of VIP receptor function [Bjurholm et al., 1992]. Surprisingly the *RANKL* gene was regulated differently in the two cell lines. At variance from the mouse periosteal osteoblasts, VIP did not affect *OPG* or *M-CSF* mRNA expression in MG-63 or SaOS-2 cells, nor did VIP affect *rankl*, *opg*, or *m-csf* mRNA expression in the rat osteosarcoma cell lines ROS 17/2.8 and UMR 106-01, although we previously have shown that UMR 106-01, but not ROS 17/2.8, express VIP receptors linked to cyclic AMP formation [Bjurholm et al., 1992]. To some extent, the differences in the responses to VIP in the different primary cells and cell lines may be due to species differences, but the heterogeneity may also be due to differences between primary cells and cell lines derived from tumor cells.

The effects of VIP on RANKL, OPG, and M-CSF in mouse periosteal osteoblasts were mediated by cyclic AMP as assessed by the finding that the effect on the expression of all these cytokines were potentiated by the cyclic AMP phosphodiesterase inhibitor rolipram. Unpublished data show that the effects of VIP were also mimicked by forskolin, stimulating adenylate cyclase, and by several cyclic AMP analogs activating protein kinase A (PKA). These observations are in line with the observation that VIP stimulates the PKA/CREB pathway in mouse calvarial osteoblasts [Persson et al., 2005]. Similarly, it has previously been reported that the stimulatory effect of parathyroid hormone (PTH) on RANKL and the inhibitory effect by the same hormone on OPG in murine stromal cells/osteoblastic cells and mouse bone marrow cells are mediated by the cyclic AMP/PKA/CREB pathway [Fu et al., 2002; Kondo et al., 2002; Lee and Lorenzo, 2002]. Previously, it has also been shown that isoproterenol stimulates RANKL expression in mouse calvarial osteoblasts and that this effect can be inhibited by the PKA inhibitor

Fig. 4. Effects of VIP and D3 on *rankl*, *opg* and *m-csf* mRNA expression in mouse bone marrow stromal cells. Bone marrow stromal cells (BMSC) were cultured in the absence (control) or presence of VIP (10^{-6} M) and D3 (10^{-9} M) for 12–120 h before RNA isolation and quantitative real-time PCR analyses of *rankl* (A), *opg* (B), and *m-csf* (C) mRNA expressions. The values for untreated cells are defined as controls and presented as 100%. Samples were analyzed in triplicates and normalized with β-actin, SEMs are shown as vertical bars when larger than the radius of the symbol.

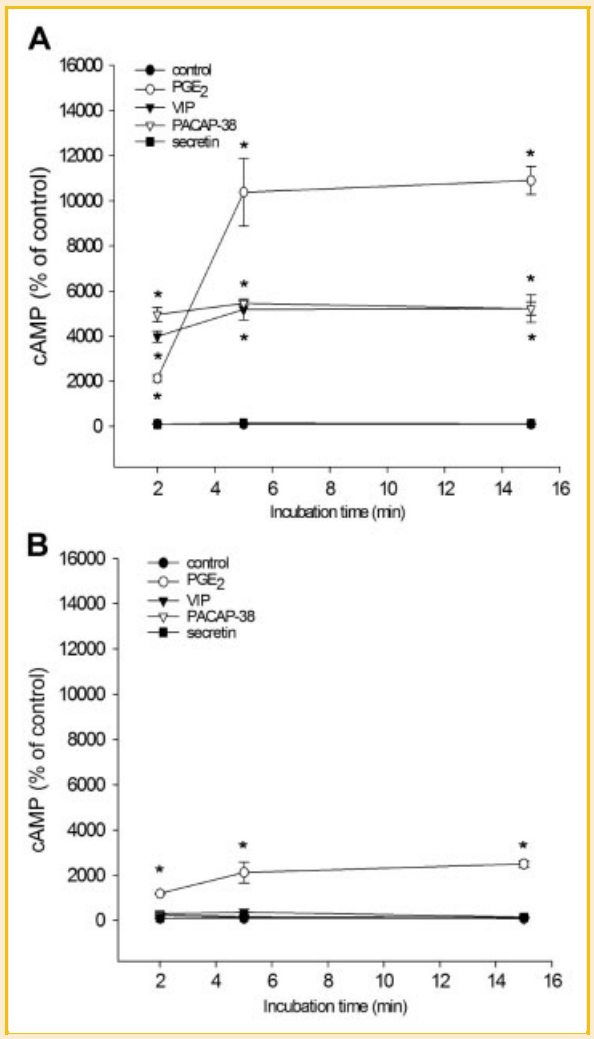

Fig. 5. Effects of VIP, PACAP-38, secretin, and PGE_2 on cyclic AMP accumulation in mouse calvarial osteoblasts (A) and mouse bone marrow stromal cells (B). Cells were incubated for 2–15 min in the absence (control) or presence of VIP, PACAP-38, secretin (all at 10^{-6} M), or PGE_2 (10^{-5} M). All cells were additionally treated with the cyclic AMP phosphodiesterase inhibitor rolipram (10^{-5} M). Values represent means for four well per group and SEMs are shown as vertical bars when larger than the height of the symbol. The values for cells treated with rolipram are defined as controls and presented as 100%. *, indicate significant difference compared to cells treated with rolipram alone, $P < 0.001$.

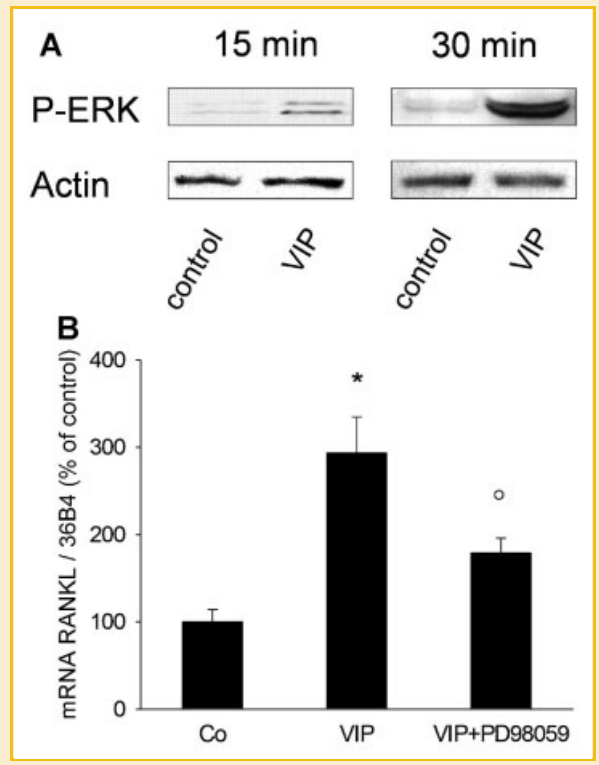

Fig. 6. The stimulatory effect by VIP on *rankl* expression in mouse calvarial osteoblasts is mediated by the MAPK/ERK pathway. Isolated calvarial osteoblasts were cultured in the absence (control) or presence of VIP (10^{-6} M) alone or in combination with the MEK1/2 inhibitor PD98059 (30 μM). A: Western blot analysis of activation through phosphorylation of ERK p42/p44 proteins. Cells were incubated for 15–30 min in the absence (control) or presence of VIP before cell lysis and subsequent Western blot analysis. The analysis was normalized through detection of actin. B: Calvarial osteoblasts were cultured in the absence (control) or presence of test substances for 48 h before RNA isolation and quantitative real-time PCR analysis of *rankl* mRNA expression. The values for untreated cells are defined as controls and presented as 100%. Samples were analyzed in triplicates and normalized with 36B4. *, indicates significant difference compared to untreated cells, $P < 0.05$. °, indicates significant difference of VIP in combination with PD98059 compared to VIP alone, $P < 0.05$.

H89 [Elefteriou et al., 2005]. However, in contrast to VIP and PTH, isoproterenol does not affect OPG expression.

Besides the involvement of cyclic AMP in the regulation by VIP of RANKL and OPG, the findings reported here indicate that the increased *rankl* mRNA expression induced by VIP is also mediated by the MEK/ERK pathway. Several previous publications have demonstrated the involvement of the MEK/ERK pathway in intracellular signaling induced by VIP. As mentioned previously, VIP has been shown to synergistically stimulate the TNF-α-induced expression of IL-6 in osteoblastic MC3T3-E1 cells [Natsume et al., 2010]. In addition, the MEK/ERK pathway has also been shown to be involved in several activities exerted by VIP in different cell types, including regulation of VEGF expression in human keratinocytes [Yu et al., 2010], and wound healing in human bronchial epithelial cells [Guan et al., 2007].

Three different subtypes of VIP receptors have been found [Vaudry et al., 2000]. VIP type 1 ($VPAC_1$) receptors recognize VIP, PACAP-38 as well as secretin, whereas $VPAC_2$ receptors show affinity to VIP and PACAP-38, but not to secretin. The third type of VIP receptors, PAC_1 receptors, has considerably higher affinity to PACAP-38 than to VIP. The fact that PACAP-38 was only 10-fold more potent than VIP as stimulator of *rankl* mRNA, and that secretin did not affect *rankl*, *opg*, or *m-csf* mRNA, indicate that the effects were mediated by PACAP preferring $VPAC_2$ receptors. This observation is in line with our previous findings using a wide variety of peptides in the VIP/secretin/glucagon family and analyzing cyclic AMP formation and radioligand binding to assess the relative potency of the different analogs [Lundberg et al., 2001]. The data also are in agreement with the finding that primary cultures of

mouse calvarial osteoblasts express $VPAC_2$, but not $VPAC_1$ or PAC_1, mRNA as assessed by semi-quantitative RT-PCR [Lundberg et al., 2001].

As expected, mouse periosteal osteoblasts responded to D3 with increased *rankl* mRNA and decreased *opg* mRNA, which is in line with the observation that D3 stimulated periosteal osteoblasts can serve as supporter cells for osteoclast formation in co-cultures with osteoclast progenitor cells [Lerner, 2004; Lorenzo et al., 2008]. In such co-cultures, BMSC can also be used as supporter cells for osteoclastogenesis and in line with this finding D3 enhanced *rankl* mRNA and decreased *opg* mRNA in mouse BMSC. In these BMSC, incubation with VIP for 12–72 h did not affect the mRNA expression of *rankl*, *opg*, or *m-csf*. The lack of effect by VIP is most likely explained by the absence of VIP receptors in BMSC as indicated by the observations that VIP and PACAP-38 did not enhance cyclic AMP accumulation in BMSC, whereas VIP and PACAP-38, but not secretin, as expected, stimulated cyclic AMP accumulation in calvarial osteoblasts.

We have previously demonstrated that VIP is a potent inhibitor of osteoclast formation in mouse bone marrow cell cultures stimulated by D3 [Mukohyama et al., 2000]. In these crude cultures, containing both mesenchymal stromal cells and hematopoetic cells, VIP reduced the stimulatory effect on *rankl* mRNA and the inhibitory effect on *opg* mRNA induced by D3. The findings in the present study indicate that these effects may be mediated by non-stromal cells present in the bone marrow.

Taken together, the observations in the present study show that VIP enhances the osteoclastogenic properties of mouse calvarial osteoblasts by increasing the RANKL/OPG ratio with no such response seen in BMSC. These data most likely explain the stimulatory effect by VIP on bone resorption reported by Hohmann et al. [1983], as demonstrated by increased release of calcium from organ cultured mouse calvarial bones.

ACKNOWLEDGMENTS

This work was supported by the Swedish Research Council for Medicine, Natural Sciences and Technology, the Swedish Rheumatism Association, the Royal 80 Year Found of King Gustav V, the County Council of Västerbotten, SalusAnsvar, and Centre for Musculoskeletal Research, University of Gävle, Umeå, Sweden. We would like to thank lab technicians Ingrid Boström, Inger Lundgren, and Anita Lie for excellent technical assistance.

REFERENCES

Bjurholm A, Kreicbergs A, Schultzberg M. 1989. Fixation and demineralization of bone tissue for immunohistochemical staining of neuropeptides. Calcif Tissue Int 45:227–231.

Bjurholm A, Kreicbergs A, Schultzberg M, Lerner UH. 1992. Neuroendocrine regulation of cyclic AMP formation in osteoblastic cell lines (UMR 106-01, ROS 17/2.8, MC3T3-E1, and SaOS-2) and primary bone cells. J Bone Miner Res 7:1011–1019.

Bjurholm A, Kreicbergs A, Terenius L, Goldstein M, Schultzberg M. 1988. Neuropeptide Y- tyrosine hydroxylase-, and vasoactive intestinal peptide-immunoreactive nerves in bone and surrounding tissues. J Auton Nerv Syst 25:119–125.

Boonekamp PM, Hekkelman JW, Hamilton JW, Cohn DV, Jilka RL. 1984. Effect of culture on the hormone responsiveness of bone cells isolated by an improved sequential digestion procedure. Proc Kon Ned Akad Wet 87:371–382.

Bucay N, Sarosi I, Dunstan CR, Morony S, Tarpley J, Capparelli C, Scully S, Tan HL, Xu W, Lacey DL, Boyle WJ, Simonet WS., 1998. Osteoprotegerin-deficient mice develop early onset osteoporosis and arterial calcification. Genes Dev 12:1260–1268.

Cherruau M, Facchinetti P, Baroukh B, Saffar JL. 1999. Chemical sympathectomy impairs bone resorption in rats: A role for the sympathetic system on bone metabolism. Bone 25:545–551.

Dai XM, Ryan GR, Hapel AJ, Dominguez MG, Russell RG, Kapp S, Sylvestre V, Stanley ER. 2002. Targeted disruption of the mouse colony-stimulating factor 1 receptor gene results in osteopetrosis, mononuclear phagocyte deficiency, increased primitive progenitor cell frequencies, and reproductive defects. Blood 99:111–120.

Dougall WC, Glaccum M, Charrier K, Rohrbach K, Brasel K, De Smedt T, Daro E, Smith J, Tometsko ME, Maliszewski CR, Armstrong A, Shen V, Bain S, Cosman D, Anderson D, Morrissey PJ, Peschon JJ, Schuh J. 1999. RANK is essential for osteoclast and lymph node development. Genes Dev 13:2412–2424.

Ducy P, Karsenty G. 2010. The two faces of serotonin in bone. J Cell Biol 191:7–13.

Elefteriou F, Ahn JD, Takeda S, Starbuck M, Yang X, Liu X, Kondo H, Richards WG, Bannon TW, Noda M, Clement K, Vaisse C, Karsenty G. 2005. Leptin regulation of bone resorption by the sympathetic nervous system and CART. Nature 434:514–520.

Fu Q, Jilka RL, Manolagas SC, O'Brien CA. 2002. Parathyroid hormone stimulates receptor activator of NF-κB ligand and inhibits osteoprotegerin expression via protein kinase A activation of cAMP-response element-binding protein. J Biol Chem 277:48868–48875.

Gray C, Hukkanen M, Konttinen YT, Terenghi G, Arnett TR, Jones SJ, Burnstock G, Polak JM. 1992. Rapid neural growth: Calcitonin gene-related peptide and substance P-containing nerves attain exceptional growth rates in regenerating deer antler. Neuroscience 50:953–963.

Guan CX, Cui YR, Zhang M, Bai HB, Khunkhun R, Fang X. 2007. Intracellular signaling molecules involved in vasoactive intestinal peptide-mediated wound healing in human bronchial epithelial cells. Peptides 28:1667–1673.

Hill EL, Elde R. 1990. An improved method for preparing cryostat sections of undecalcified bone for multiple uses. J Histochem Cytochem 38:443–448.

Hill EL, Elde R. 1991. Distribution of CGRP-, VIP-, DβH-, and NPY-immunoreactive nerves in the periosteum of rat. Cell Tissue Res 264:469–480.

Hohmann EL, Tashjian, AH. Jr. 1984. Functional receptors for vasoactive intestinal peptide on human osteosarcoma cells. Endocrinology 114:1321–1327.

Hohmann EL, Elde RP, Rysavy JA, Einzig S, Gebhard RL. 1986. Innervation of periosteum and bone by sympathetic vasoactive intestinal peptide-containing nerve fibers. Science 232:868–871.

Hohmann EL, Levine L, Tashjian, AH. Jr. 1983. Vasoactive intestinal peptide stimulates bone resorption by a cyclic adenosine 3′,5′-monophosphate-dependent mechanism. Endocrinology 112:1233–1239.

Hughes AE, Ralston SH, Marken J, Bell C, MacPherson H, Wallace RG, van Hul W, Whyte MP, Nakatsuka K, Hovy L, Anderson DM. 2000. Mutations in TNFRSF11A, affecting the signal peptide of RANK, cause familial expansile osteolysis. Nature Genet 24:45–48.

Hukkanen M, Konttinen YT, Rees G, Santavirta S, Terenghi G, Polak JM. 1993. Distribution of nerve endings and sensory neuropeptides in the rat synovium, meniscus, and bone. Int J Tissue React 14:1–10.

Imai S, Rauvala H, Konttinen YT, Tokunaga T, Maeda T, Hukuda S, Santavirta S. 1997. Efferent targets of osseous CGRP-immunoreactive nerve fiber before and after bone destruction in adjuvant arthritic rat: An

ultramorphological study on their terminal-target relations. J Bone Miner Res 12:1018–1027.

Johnson-Pais TL, Singer FR, Bone HG, McMurray CT, Hansen MF, Leach RJ. 2003. Identification of a novel tandem duplication in exon 1 of the TNFRSF11A gene in two unrelated patients with familial expansile osteolysis. J Bone Miner Res 18:376–380.

Kondo H, Guo J, Bringhurst FR. 2002. Cyclic adenosine monophosphate/protein kinase A mediates parathyroid hormone/parathyroid hormone-related protein receptor regulation of osteoclastogenesis and expression of RANKL and osteoprotegerin mRNAs by marrow stromal cells. J Bone Miner Res 17:1667–1679.

Kong YY, Yoshida H, Sarosi I, Tan HL, Timms E, Capparelli C, Morony S, Oliveira-dos-Santos AJ, Van G, Itie A, Khoo W, Wakeham A, Dunstan CR, Lacey DL, Mak TW, Boyle WJ, Penninger JM., 1999. OPGL is a key regulator of osteoclastogenesis, lymphocyte development and lymph-node organogenesis. Nature 397:315–323.

Lee SK, Lorenzo JA. 2002. Regulation of receptor activator of nuclear factor-kappa B ligand and osteoprotegerin mRNA expression by parathyroid hormone is predominantly mediated by the protein kinase A pathway in murine bone marrow cultures. Bone 31:252–259.

Lerner UH. 2004. New molecules in the tumor necrosis factor ligand and receptor superfamilies with importance for physiological and pathological bone resorption. Crit Rev Oral Biol Med 15:64–81.

Lerner UH, Persson E, Lundberg P. 2008. Kinins and neuro-osteogenic factors. In: Bilezikian JP, Raisz LG, Rodan GA, editors. Principles of bone biology, 3rd edn. San Diego: Academic Press. pp 1025–1057.

Lerner UH, Lundberg P, Ransjö M, Persson P, Håkansson R. 1994. Helodermin, helospectin, and PACAP stimulate cyclic AMP formation in intact bone, isolated osteoblasts, and osteoblastic cell lines. Calcif Tissue Int 54:284–289.

Lorenzo J, Horowitz M, Choi Y. 2008. Osteoimmunology: Interactions of the bone and immune system. Endocr Rev 29:403–440.

Lundberg P, Boström I, Mukohyama H, Bjurholm A, Smans K, Lerner UH. 1999. Neuro-hormonal control of bone metabolism: Vasoactive intestinal peptide stimulates alkaline phosphatase activity and mRNA expression in mouse calvarial osteoblasts as well as calcium accumulation in mineralized bone nodules. Regul Peptides 85:47–58.

Lundberg P, Lie A, Bjurholm A, Lehenkari PP, Horton MA, Lerner UH, Ransjö M. 2000. Vasoactive intestinal peptide binds to bone cells and regulates osteoclast activity. Bone 27:803–810.

Lundberg P, Lundgren I, Mukohyama H, Lehenkari PP, Horton MA, Lerner UH. 2001. VIP/PACAP receptor subtypes in mouse calvarial osteoblasts: Presence of VIP-2 receptors and differentiation-induced expression of VIP-1 receptors. Endocrinology 142:339–347.

Madsen JE, Hukkanen M, Aune AK, Basran I, Möller JF, Polak JM, Nordsletten L. 1998. Fracture healing and callus innervation after peripheral nerve resection in rats. Clin Orthop Rel Res 351:230–240.

Mukohyama H, Ransjö M, Taniguchi H, Ohyama T, Lerner UH. 2000. The inhibitory effects of vasoactive intestinal peptide and pituitary adenylate cyclase-activating polypeptide on osteoclast formation are associated with upregulation of osteoprotegerin and downregulation of RANKL and RANK. Biochem Biophys Res Commun 271:158–163.

Nakashima T, Takayanagi H. 2009. Osteoclasts and the immune system. J Bone Miner Metab 27:519–529.

Natsume H, Tokuda H, Mizutani J, Adachi S, Matsushima-Nishiwaki R, Minamitani C, Kato K, Kozawa O, Otsuka T. 2010. Synergistic effect of vasoactive intestinal peptide on TNF-alpha-induced IL-6 synthesis in osteoblasts: Amplification of p44/p42 MAP kinase activation. Int J Mol Med 25:813–817.

Persson E, Lerner UH. 2005. The neuropeptide VIP potentiates IL-6 production induced by proinflammatory osteotropic cytokines in calvarial osteoblasts and the osteoblastic cell line MC3T3-E1. Biochem Biophys Res Commun 335:705–711.

Persson E, Voznesensky OS, Huang YF, Lerner UH. 2005. Increased expression of interleukin-6 by vasoactive intestinal peptide is associated with regulation of CREB, AP-1, and C/EBP, but not NF-κB, in mouse calvarial osteoblasts. Bone 37:513–529.

Ransjö M, Lie A, Mukohyama H, Lundberg P, Lerner UH. 2000. Microisolated mouse osteoclasts express VIP-1 and PACAP receptors. Biochem Biophys Res Commun 274:400–404.

Ross FP, Teitelbaum SL. 2005. αvβ3 and macrophage colony-stimulating factor: Partners in osteoclast biology. Immunol Rev 208:88–105.

Togari A, Arai M, Mizutani S, Koshihara Y, Nagatsu T. 1997. Expression of mRNAs for neuropeptide receptors and beta-adrenergic receptors in human osteoblasts and human osteogenic sarcoma cells. Neurosci Lett 19:125–128.

Vaudry D, Gonzalez BJ, Basille M, Yon L, Fournier A, Vaudry H. 2000. Pituitary adenylate cyclase-activating polypeptide and its receptors: From structure to functions. Pharmacol Rev 52:269–324.

Whyte MP, Hughes AE., 2002. Expansile skeletal hyperphosphatasia is caused by a 15-base pair tandem duplication in TNFRSF11A encoding RANK and is allelic to familial expansile osteolysis. J Bone Miner Res 17:26–29.

Whyte MP, Obrecht SE, Finnegan PM, Jones JL, Podgornik MN, McAlister WH, Mumm S., 2002. Osteoprotegerin deficiency and juvenile Paget's disease. New Engl J Med 347:175–184.

Wong IP, Zengin A, Herzog H, Baldock PA., 2008. Central regulation of bone mass. Semin Cell Dev Biol 19:452–458.

Yadav VK, Oury F, Suda N, Liu ZW, Gao, XB, Canfavreux C, Klemenhagen KC, Tanaka KF, Gingrich JA, Guo XE, Tecott LH, Mann JJ, Hen R, Horvath TL, Karsenty G., 2009. A serotonin-dependent mechanism explains the leptin regulation of bone mass, appetite, and energy expenditure. Cell 138:976–989.

Yoshida H, Hayashi S, Kunisada T, Ogawa M, Nishikawa S, Okamura H, Sudo T, Shultz LD, Nishikawa S., 1990. The murine mutation osteopetrosis is in the coding region of the macrophage colony stimulating factor gene. Nature 345:442–444.

Yu XJ, Ren XH, Xu YH, Chen LM, Zhou CL, Li CY., 2010. Vasoactive intestinal peptide induces vascular endothelial growth factor production in human HaCaT keratinocytes via MAPK pathway. Neuropeptides 44:407–411.